WORLD CONFERENCE ON TIMBER ENGINEERING 2025
BRISBANE, AUSTRALIA
Advancing Timber for the Future Built Environment

PARAMETRIC STUDY ON THE BENDING PERFORMANCE OF WOODEN DOWELS

Inayat Ullah Khan [1], Mahbube Subhani [2], Kazem Ghabraie [3], Mahmud Ashraf [4]

ABSTRACT: Wooden dowels serve as the primary connecting elements in dowel-laminated timber (DLT), and their mechanical performance directly influences the structural integrity of DLT systems. Therefore, accurate characterisation of the mechanical properties of wooden dowels is essential. Timber-to-timber connections are designed following standards such as the National Design Specification (NDS) and Eurocode 5, which require the dowel yield moment or bending yield strength as input parameters. However, these standards are primarily based on the testing of metal dowels, which cannot be directly applied to wooden dowels due to their lower stiffness and susceptibility to localized deformation. This study experimentally investigates the bending behaviour of Australian hardwood dowels, specifically Tasmanian Oak dowels with a 19 mm diameter. The experimental results are numerically validated using the material model MAT-143 in LS-DYNA. Various support conditions are analysed to minimize their influence on the measured bending properties, both experimentally and numerically. A parametric study is also conducted by varying the dowel diameter, leading to the development of an empirical equation for predicting the maximum load and yield moment of dowels in bending. The results indicate that the bending yield moment increases with dowel diameter. This study provides valuable insights for researchers and engineers seeking to assess the bending performance of wooden dowels in structural applications.

KEYWORDS: LS-DYNA, wooden dowels, Tasmanian Oak, Bending, MAT-143

1 – INTRODUCTION

Sawn timber elements are joined using either mechanical fasteners or adhesives to manufacture engineered timber products (ETPs). However, the widespread use of adhesives and metal fasteners in ETPs poses challenges related to reusability, end-of-life disposal, recyclability, and automated processing. Adhesives, particularly those containing formaldehyde, raise environmental concerns [1]. Their application requires strict control over parameters such as pressure, curing time, and temperature, making the process complex. Additionally, in high-density timber, achieving effective bonding can be challenging, often necessitating surface preparation prior to adhesive application [2]. To address these limitations, wooden dowels have been introduced for the production of dowel-laminated timber (DLT), an adhesive-free alternative. DLT is well-suited for Computer Numerical Control (CNC) machining, which has facilitated its industrial adoption. StructureCraft, a leading North American manufacturer, operates the world's largest automated DLT production line. Unlike metal-based laminated timber, DLT does not cause significant wear on cutting tools, and its recyclability is enhanced due to the absence of metal fasteners [3]. In DLT and other wooden dowel connections, load resistance is primarily governed by the dowels' bending strength, cross-shear resistance, and embedment resistance.

Current design standards, such as Eurocode 5 [4] and the National Design Specification (NDS) [5], are primarily developed for joints with metal fasteners and provide formulations for evaluating their load-bearing capacity. However, wooden joints utilising wooden dowels remain an area of ongoing research, and no standardized design guidelines have been established. The bending performance of wooden dowels is particularly critical for slender dowels, where load resistance in the joint occurs through the formation of plastic hinges. This makes bending strength a key parameter in assessing the structural capacity of wooden dowel joints. The yield moment and bending yield strength of dowels are essential for designing timber-to-timber connections and serve as input parameters in the yield limit equations of Eurocode 5 and NDS for timber joint design. Consequently, a comprehensive understanding of the bending behaviour of wooden dowels is fundamental to advancing the design and implementation of dowel-based timber connections.

[1] Inayat Ullah Khan, School of Engineering, Deakin University, Waurn Ponds, VIC, Australia, inayat.khan@deakin.edu.au

[2] Mahbube Subhani, School of Engineering,Deakin University,Waurn Ponds, VIC, Australia, mahbube.subhani@deakin.edu.au

[3] Kazem Ghabraie, School of Engineering, Deakin University, Waurn Ponds, VIC, Australia, k.ghabraie@deakin.edu.au

[4] Mahmud Ashraf, School of Engineering, Deakin University, Waurn Ponds, VIC, Australia, mahmud.ashraf@deakin.edu.au

https://doi.org/10.52202/080513-0351

Hardwood dowels exhibit superior mechanical properties, making them a more effective choice as connecting elements in timber structures. Australia has an extensive forested area of 133.6 million hectares, with native forests comprising 98% of this total. Notably, approximately 77% of the native forest consists of hardwood species, presenting significant potential for hardwood applications, including their use as wooden dowels in timber-to-timber connections [6].

Despite this potential, the bending performance of Australian hardwood dowels, particularly Tasmanian Oak (TO), has not been extensively studied, especially concerning the parameters influencing their mechanical behaviour. In this study, Tasmanian Oak dowels were experimentally tested under bending, and the results were validated using the continuum damage mechanics (CDM)-based material model MAT-143 in LS-DYNA. Furthermore, traditional timber-to-timber connection design approaches rely primarily on the elastic properties of timber, without accounting for post-elastic or fracture behaviour. To address this limitation, MAT-143 was utilised to investigate the post-elastic force-deformation response of timber using fracture energy-based modelling. Following model validation, the influence of dowel diameter on bending properties was evaluated. This study provides valuable insights into the mechanical characterisation of wooden dowels and will serve as a useful reference for researchers and engineers working in the field of timber connections.

2 – EXPERIMENTAL SETUP

Tasmanian Oak (TO) dowels, sourced from the market with an initial length exceeding 2 meters, were cut to the required dimensions using a mitre saw. The moisture content (MC) was measured using a protimeter at three stages: prior to conditioning, after conditioning, and immediately after testing near the failure zone. The initial MC measurement provided an estimate for the required conditioning duration. Dowels with an MC close to 12% were conditioned for a shorter duration, while others remained in the conditioning chamber until reaching an MC of 12%.

The dowels used in this study had a diameter of 19 mm and a length of 200 mm. The measured density was 650 kg/m³, with an oven-dry specific gravity of 0.631. ASTM D8023-23 [7] specifies a minimum oven-dry specific gravity of 0.570 for wooden dowels, which the tested dowels met. Additionally, the dowels exhibited parallel grain alignment and were free from defects such as shakes, knots, or splits, in compliance with ASTM D8023-23.

Currently, no specific standard governs the bending testing of wooden dowels. However, ASTM F1575-24 [8] recommends a span of 11.5 times the dowel diameter for dowels with a diameter exceeding 4.83 mm. Due to the inherent variability in wood properties, further studies are required to establish standardized guidelines for the bending testing of wooden dowels. In this study, a total span of 200 mm with a central span of 150 mm was used. The load was applied at a displacement rate of 5 mm/min. The bending yield moment and bending yield strength were calculated using Equations (1) and (2), as per ASTM F1575.

$$M_y = \frac{PL}{4} \tag{1}$$

$$F_{yb} = \frac{M_y}{Z} = \frac{6M_y}{D^3} \tag{2}$$

Where
L= Span of dowel (150mm)
P = Yield load determined as per 5% offset line
D = Dowe diameter
Z= Plastic section modulus
M_y= Yield moment
F_{yb}= Bending yield strength

The yield load was determined following the procedure illustrated in Figure 1, by drawing a line parallel to the linear portion of the force-deformation curve at an offset of 5% of the dowel diameter. This standard specifies the use of circular supports and loading points with a diameter of 9.53 mm. The test was conducted using two different support configurations, as shown in Figure 2. The 5% offset method is specifically designed for metal dowels, and its applicability to wooden dowels requires further investigation. Due to the inherent variability in wood properties, the force-deformation behaviour of wooden dowels can differ significantly, potentially making the 5% offset method unreliable for determining yield load. This limitation has also been discussed by Hindman in his report [9].

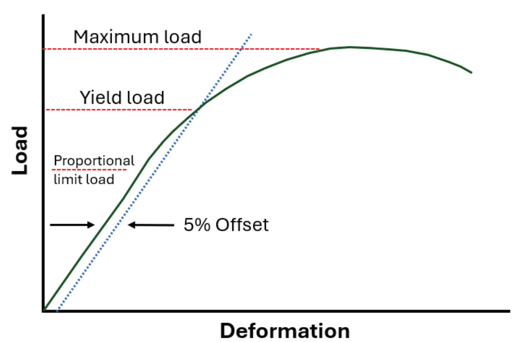

Figure 1 Load-deformation curve from dowel bending test

https://doi.org/10.52202/080513-0351

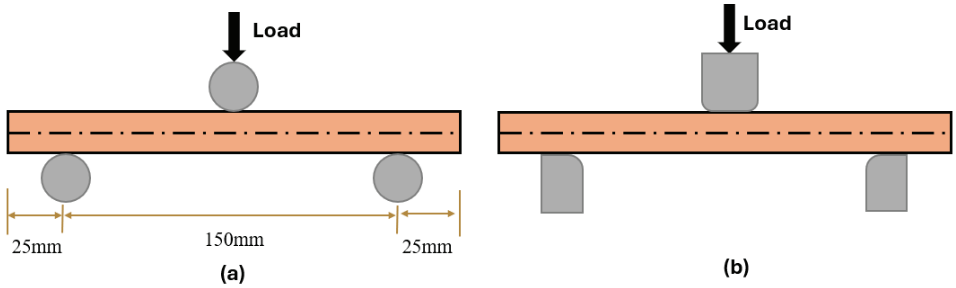

Figure 2 Supports types (a) Circular by ASTM F1575 (b) Rectangular with chamfered edges

3 – NUMERICAL MODELING

LS-DYNA was used for numerical modelling due to its extensive library of built-in material models, including those specifically designed for wood. Among the more than 250 available material models, MAT-143 was selected for this study. Unlike other LS-DYNA models primarily developed for fibre-reinforced composite materials, MAT-143 is tailored for wood, with input parameters that can be obtained experimentally. While fibre composite-based material models can also be used for wood, they require complex input parameters such as delamination properties between the matrix and fibres, which are challenging to determine for natural materials like wood.

MAT-143 is a transversely isotropic material model, assuming identical radial and tangential properties for timber. The model requires various input parameters, including density, elastic moduli, material strengths, softening parameters, damage parameters, hardening parameters, and fracture energies. To enhance understanding, some key theoretical aspects of MAT-143 are discussed. This model integrates multiple formulations to create a comprehensive representation of wood behaviour, including elastic constitutive equations, failure criteria, plastic flow, hardening, post-peak softening, and strain rate effects. It requires five primary elastic constants: E_L, E_T, G_{LT}, G_{TR} and υ_{LT}.

The failure criteria were defined based on strength using modified Hashin's formulations. Two types of failures modes were defined, parallel to grain and perpendicular to grain. For parallel, failure occurs when $f_{\parallel} \geq 0$ and for perpendicular occurs when $f_{\perp} \geq 0$.

$$f_{\parallel} = \frac{{\sigma_{11}}^2}{X^2} + \frac{({\sigma_{12}}^2 + {\sigma_{13}}^2)}{{S_{\parallel}}^2} - 1 \qquad (3)$$

$$f_{\parallel} = \frac{(\sigma_{22} + \sigma_{33})^2}{Y^2} + \frac{({\sigma_{23}}^2 - \sigma_{22}\sigma_{33})}{{S_{\perp}}^2} - 1 \qquad (4)$$

Where X is strength parallel to grain which is $X=X_T$ when $\sigma_{11} > 0$ and $X=X_C$ when $\sigma_{11} < 0$. Where Y is strength perpendicular to grain which is $Y=Y_T$ when $\sigma_{22} + \sigma_{33} > 0$ and $Y=Y_C$ when $\sigma_{22} + \sigma_{33} < 0$. These equations can be also presented in form of stress invariants such as $I_1 = \sigma_{11}$, $I_4 = {\sigma_{12}}^2 + {\sigma_{13}}^2$, $I_2 = \sigma_{22} + \sigma_{33}$ and $I_3 = {\sigma_{23}}^2 - \sigma_{22}\sigma_{33}$

Once the failure criteria as per equation 5 and 6 is satisfied, the plasticity algorithm constraint the stress component. Based on traditional approach for modelling plasticity, is to divide stress and strain into elastic and plastic components. Partitioning is performed using return mapping algorithm that impose the plastic consistency condition. Due to presence of two modes, one parallel and other perpendicular, separate plasticity algorithm is modelled for each by enforcing separate consistency conditions such as $\Delta\lambda_{\parallel}$ and $\Delta\lambda_{\perp}$.

$$\Delta\lambda_{\parallel} = \frac{-{f_{\parallel}}^*}{\left.\frac{\partial f_{\parallel}}{\partial I_1}\right|_n \left.\frac{\partial I_1}{\partial \lambda_{\parallel}}\right|_n + \left.\frac{\partial f_{\parallel}}{\partial I_4}\right|_n \left.\frac{\partial I_4}{\partial \lambda_{\parallel}}\right|_n} \qquad (5)$$

$$\Delta\lambda_{\perp} = \frac{-{f_{\perp}}^*}{\left.\frac{\partial f_{\perp}}{\partial I_2}\right|_n \left.\frac{\partial I_2}{\partial \lambda_{\perp}}\right|_n + \left.\frac{\partial f_{\perp}}{\partial I_3}\right|_n \left.\frac{\partial I_3}{\partial \lambda_{\perp}}\right|_n} \qquad (6)$$

$\Delta\lambda_{\parallel}$ and $\Delta\lambda_{\perp}$ is determined using the total strain increments and the yield functions ${f_{\parallel}}^* = f_{\parallel}({I_1}^*, {I_4}^*)$ and ${f_{\perp}}^* = f_{\perp}({I_2}^*, {I_3}^*)$, respectively. The trial elastic stress invariants ${I_1}^*, {I_2}^*$, ${I_3}^*$, and ${I_4}^*$ are determined from the trial elastic stresses σ^*. Stresses updates are performed using the total strain increments and the consistency parameters as follows

$$\sigma = \sigma^* - C\Delta\lambda \frac{\partial f}{\partial \sigma} \qquad (7)$$

In case of normal stress, each update depends on the consistency parameters and yield surface formulations for both the parallel [$\Delta\lambda = \Delta\lambda_{\parallel}$ and $f = f_{\parallel}$] and perpendicular modes [$\Delta\lambda = \Delta\lambda_{\perp}$ and $f = f_{\perp}$]. The translation of yield surfaces is illustrated in Figure 3, while the input parameters required for MAT-143 are summarized in table 1. The density, strength, and elastic modulus of Tasmanian Oak (TO) dowels were determined experimentally through extensive testing. These results are currently under review in journal publications and are presented here solely for modelling purposes. Softening and hardening parameters were derived from experimental force-deformation curves with the aid of single-element simulations. MAT-143 requires four hardening parameters: NPAR, CPAR, NPER, and CPER, where PAR denotes the parallel direction and PER represents the perpendicular direction. The parameters C‖ and C⊥ control the rate of hardening, with smaller values resulting in gradual hardening and larger values leading to steeper hardening. Similarly, N‖ and N⊥ define the fraction of the ultimate strength at which nonlinear behaviour begins. For instance, N = 0.4 implies that nonlinearity initiates at 60% of the ultimate strength. Fracture energy values for dowels were obtained from existing literature [10], [11], [12]. The damage parameters were set as DMAX‖ = 0.9999 and DMAX⊥ = 0.9900, where $d = 0$ indicates no damage and $d = 1$ represents complete failure. These values are intentionally set slightly below 1 to prevent computational difficulties associated with zero stiffness.

For a more detailed understanding of MAT-143, readers are encouraged to refer to the LS-DYNA manuals [11], [12].

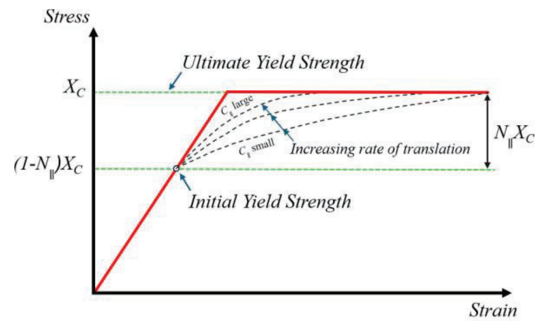

Figure 3 Translating yield surfaces with hardening

Table 1 Data card for MAT-143

RO	Mass density	650×10^{-9}	kg/mm^3
EL	Parallel normal modulus	4.99	GPa
ET	Perpendicular normal modulus	0.350	GPa
GLT=GLR	Parallel shear modulus	1.9280	GPa
GTR	Perpendicular shear modulus	0.400	GPa
PR	Parallel major Poisson's ratio	0.1800	
XT	Parallel tensile strength	0.14262	GPa
XC	Parallel compressive strength	0.07398	GPa
YT	Perpendicular tensile strength	0.00433	GPa
YC	Perpendicular compressive strength	0.008401	GPa
SXY	Parallel shear strength	0.01343	GPa
SYZ	Perpendicular shear strength	0.01343	GPa
GF1‖	Parallel fracture energy in tension	0.0200	GPa.mm
GF2‖	Parallel fracture energy in shear	0.1115	GPa.mm
BFIT	Parallel softening parameter.	300	
DMAX‖	Parallel maximum damage.	0.9999	
GF1P	Perpendicular fracture energy in tension	0.00101	GPa.mm
GF2P	Perpendicular fracture energy in shear	0.00165	GPa.mm
DFIT	Perpendicular softening parameter	300	
DMAXP	Perpendicular maximum damage	0.99	
NPAR	Parallel hardening initiation	0.400	
CPAR	Parallel hardening rate	850	
NPER	Perpendicular hardening initiation	0.500	
CPER	Perpendicular hardening rate	250.0	

https://doi.org/10.52202/080513-0351

The dowel geometry developed in LS-DYNA is illustrated in Figure 4. Two supports (left and right) and a loading punch were modelled as rigid bodies using the MAT_020 (Rigid) material model, with material properties corresponding to steel. A mesh sensitivity analysis was performed, as shown in Figure 5, indicating that a 2 mm mesh size provided results in reasonable agreement with experimental data while maintaining computational efficiency. Although a 1 mm mesh size yielded highly accurate results, it significantly increased computational time. The interaction between the supports, loading punch, and dowels was defined using AUTOMATIC_SURFACE_TO_SURFACE_CONTACT to ensure proper load transfer and realistic interaction behaviour. Initially, a 19 mm dowel was modelled, followed by a parametric study to investigate the effect of dowel diameter by analysing 9.5 mm and 16 mm dowels under different support conditions.

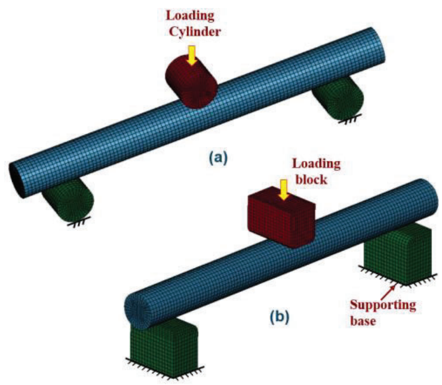

Figure 4 Bending test of dowel with (a) circular (b) Chamfered rectangular support

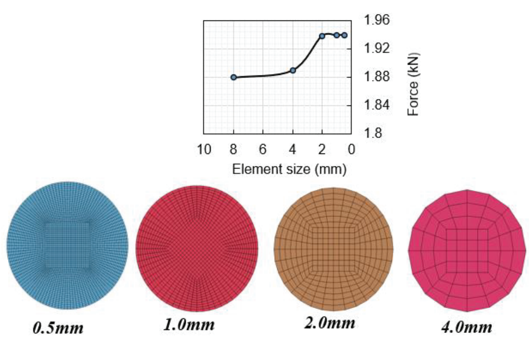

Figure 5 Effect of mesh size on max load

4 – RESULTS

Deformation and load measurements were taken at the centre of the dowel beam and are presented in Figure 6. The force-deformation response of Tasmanian Oak under bending consists of three main regions. The first region is the linear-elastic phase, where force increases proportionally with displacement. The second region, where non-linearity begins, is characterized by a reduced rate of force increase relative to displacement. This stage, known as the hardening region, continues until the load reaches its peak. Non-linearity starts to develop in the displacement range of 3.5 to 4 mm, gradually intensifying until peak load is reached.

The third region is the softening phase, where force decreases as displacement increases. However, this decrease occurs in progressive steps. Since wood consists of fibres aligned in the longitudinal direction, the bending process places the bottom fibres under tension and the top fibres under compression. When the tensile stress in the bottommost fibres reaches their capacity, they fracture, transferring the load to the adjacent fibres above them. This redistribution mechanism temporarily increases the load until the next set of fibres fractures, causing a subsequent drop in force. This alternating increase and decrease in force continue in a stepwise manner throughout the softening phase.

Experimental results were compared with numerical simulations, showing a strong correlation between the two. The key results from the force-deformation curves are summarized in table 2, where the difference between experimental and numerical values remains within 4%. The bending capacity was determined following the ASTM F1575 [8] guidelines. The failure of the dowels occurred primarily at mid-tension with slight longitudinal shear. The dowel failure modes are illustrated in Figure 7.

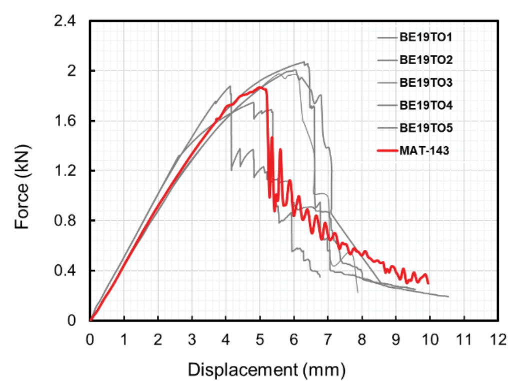

Figure 6 Force-deformation curves for dowel bending

Table 2 Results from bending test

ID	Yield Load (kN)	M_y (kN.mm)	F_{yb} (MPa)	E_b (MPa)
TO1	1.92	72	62.98	4647.30
TO2	1.52	57	49.86	5478.04
TO3	1.92	72	62.98	4512.78
TO4	1.68	63	55.11	5617.80
TO5	1.96	73.5	64.30	4710.74
Average	1.80	67.50	59.05	4993.32
COV %	10.66	10.66	10.66	10.29
MAT-143	1.87	70.13	61.34	4793.50
Exp/ Num	0.96	0.96	0.96	1.04

Figure 7 Dowel failure under bending

The dowels were initially modelled with a 19 mm diameter to compare the numerical results with experimental data using the MAT-143 material model. After validating the results, the effect of dowel diameter on maximum load and yield moment was evaluated using three different diameters. The results are presented in Figure 8. It can be observed that both maximum load and yield moment increase with increasing dowel diameter. Furthermore, a power-law empirical equation was used to fit the data, yielding an R^2 value between 0.97 and 0.98, indicating a strong correlation between the parameters.

The effect of dowel strength on local compression was evaluated through experimental testing and finite element simulations using LS-DYNA. It was found that increasing the strength and elastic modulus of the dowels reduced local compression. Since steel is nearly 15 times denser than wood, this significant difference led to local compression of wood at the supports and load application points. Given that this study involved hardwood dowels, even greater local compression is expected when testing low-density dowels.

Rectangular chamfered supports performed well with hardwood dowels. However, for dowels made of lower stiffness materials, even rectangular chamfered supports resulted in local compression. Figure 9 shows that using circular supports with dowels causes local compression, which reduces the measured strength and elastic modulus. The chamfered support specimens resisted 1.38 times more load than the circular support specimens. The reason for this is that circular supports concentrate force on a small area, leading to local compression and reducing the bending strength and flexural modulus. In contrast, rectangular supports with chamfered edges distribute the load more evenly, minimizing indentation and allowing for a more accurate assessment of flexural properties.

Local compression reduces the effective bending section of the dowel. Figure 10a shows results where the dowel properties were doubled compared to the values in table 1. Although smaller circular supports and load points were used, no local compression was observed. Figure 10b also shows effective performance with chamfered supports, using the current study's data. Neglible indentation was observed. In contrast, Figure 10c, where half the current dowel property values were used, clearly demonstrates local compression. The deformation observed in the steel block in Figure 10c represents indentation in the wooden dowel. Only the block moved downward with minimal deformation of the dowel. This highlights the importance of choosing appropriate supports when testing wooden dowels, based on their mechanical properties. Boli et al. [10] used densified wood dowels with metal supports but did not report local compression, as the improved properties of densified wood dowels made them more compatible with the supports. However, the issue becomes more severe when using low-stiffness dowels. This explains why ASTM F1575 [8] recommends circular supports and load application points for metal dowels, as metal dowels are significantly stiffer and less prone to local compression effects.

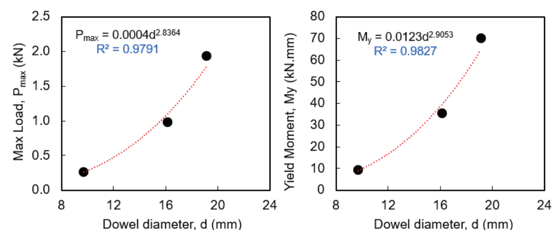

Figure 8 Maximum load and yield moment variation with dowel size

Figure 9 Local compression at load application point

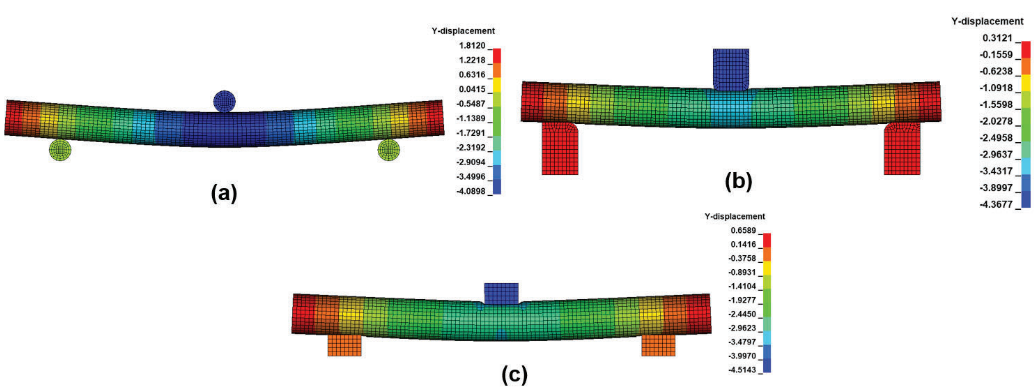

Figure 10 Dowel bending with properties (a) Double (b) Equal (c) Half, of the current study

https://doi.org/10.52202/080513-0351

5 – CONCLUSION

In this study, Australian hardwood dowels made of Tasmanian Oak with a diameter of 19 mm were tested in bending, and the results were analysed for yield load, yield moment, bending yield strength, and bending modulus. The Tasmanian Oak dowel was also modelled using the material model MAT-143 in LS-DYNA.

- The yield load, yield moment, bending yield strength, and flexural modulus of Tasmanian Oak were found to be 1.80 kN, 67.50 kN·mm, 59.05 MPa, and 4993.32 MPa, respectively, with a coefficient of variation of 10 percent.
- MAT-143 accurately captured the bending behaviour of the dowel, with a maximum difference of 4 percent between experimental and numerical results. Additionally, the material model effectively represented the force-deformation response across all stages, including the linear portion, hardening, peak, and softening phases.
- The maximum load and yield moment obtained from bending tests showed a strong positive correlation with dowel size for a given material property and dowel length, with an R^2 value ranging from 0.97 to 0.98.
- Local compression decreased with increasing dowel strength and stiffness. Round chamfered supports were suitable for low-strength dowels, while circular supports performed better for high-strength dowels, such as densified dowels.

These findings will be valuable for researchers and engineers working on the numerical modelling or analytical study of dowel-laminated timber using Tasmanian Oak dowels. Given the significant difference in properties between wooden dowels and steel supports or load application crossheads, local compression consistently occurs at their contact points. Future studies could focus on the effect of dowel length on bending properties, with and without considering shear deformation.

REFERENCES

[1] A. Sotayo *et al.*, "Review of state of the art of dowel laminated timber members and densified wood materials as sustainable engineered wood products for construction and building applications," *Dev. Built Environ.*, vol. 1, p. 100004, Feb. 2020, doi: 10.1016/j.dibe.2019.100004.

[2] L. Adamčík, L. Dzurenda, A. Banski, and R. Kminiak, "Comparison of Surface Roughness of Beech Wood after Sanding with an Eccentric and Belt Sander," *Forests*, vol. 15, no. 1, Art. no. 1, Jan. 2024, doi: 10.3390/f15010045.

[3] StructureCraft, "Dowel Laminated Timber, The All-Wood Mass Timber Panel," StructureCraft. Accessed: Dec. 22, 2024. [Online]. Available: https://structurecraft.com/materials/mass-timber/dlt-dowel-laminated-timber

[4] CEN, *EN 1995-1-1 (2004) (English): Eurocode 5: Design of timber structures - Part 1-1: General - Common rules and rules for buildings*, Jun. 2008.

[5] American Forest & Paper Association, *ANSI/AF&PA NDS-2012 National Design Specification for Wood Construction*, AF&PA, Washington, D.C.,., 2012.

[6] Department of Agriculture, Fisheries and Forestry, "Australia's forests – overview - DAFF." Accessed: Jun. 25, 2024. [Online]. Available: https://www.agriculture.gov.au/abares/forestsaustralia/australias-forests/profiles/australias-forests-2019

[7] D07 Committee, *ASTM D8023-23 Specification for Round Wood Dowels (Pegs) for Use in Wood Construction*, 100 Barr Harbor Drive, PO Box C700, West Conshohocken, PA, 19428-2959 USA., 2023. doi: 10.1520/D8023-23.

[8] ASTM F1575/F1575M, *Standard Test Method for Determining Bending Yield Moment of Nails, Spikes, and Dowel-type Threaded Fasteners*, Mar. 20, 2024. doi: 10.1520/F1575_F1575M-24.

[9] D. Hindman, "Measuring the bending yield strength of timber frame pegs," Department of Sustainable Biomaterials, Virginia Tech, Jan. 2017.

[10] G. B. D. B. Boli, M.-G. Tétreault, M. Oudjene, D. Coutellier, H. Naceur, and M. Fafard, "Numerical modelling of the structural response of a novel hybrid densified wood filled-aluminium tube dowel for structural timber connections," *Compos. Struct.*, vol. 334, p. 117987, Apr. 2024, doi: 10.1016/j.compstruct.2024.117987.

[11] Y. D. Murray, "Manual for LS-DYNA Wood Material Model 143," APTEK, Inc. 1257 Lake Plaza Drive Colorado Springs, CO 80906-3558, FHWA-HRT-04-097, Aug. 2007. Accessed: Jul. 27, 2024. [Online]. Available: https://www.fhwa.dot.gov/publications/research/safety/04097/04097.pdf

[12] Y. D. Murray, J. D. Reid, R. K. Faller, and B. W. Bielenberg, "Evaluation of LS-DYNA Wood Material Model 143.," Aptek, Inc., Colorado Springs, CO.; Nebraska Univ.-Lincoln. Midwest Roadside Safety Facility.; John A. Volpe National Transportation Systems Center, Cambridge, MA., PB2006101279, 2005. Accessed: Dec. 16, 2024. [Online]. Available: https://ntrl.ntis.gov/NTRL/dashboard/searchResults/titleDetail/PB2006101279.xhtml